2021 SCEC Annual Report #21087
Shallow Elastic Structure in the upper 100 m from Colocated Seismic and Pressure Data
Period: 2/1/2021-1/31/2022

PI : Toshiro Tanimoto (UC Santa Barbara)

1.Project Objective

We developed and have been improving an inversion method for deriving shallow elastic structure based on analysis of co-located pressure and seismic data. The method analyzes quasi-static deformation, part of seismic noise caused by large surface pressure variations for frequencies between 0.01 Hz and 0.05 Hz It is a new method, although the phenomenon was noted since around 1970. Co-located stations have rapidly increased in the last 10 years, including the EarthScope Transportable Array. We have tested the method by comparing our results for Vs30 against independent Vs30 measurements. During 2021, we applied this inversion method to some other colocated stations in Southern California from 2000.

2.Method and Background Phenomenon

(2.1) Background

In the frequency range 0.01-0.05 Hz, surface pressure variations often show high coherence with seismic ground motions. Figure 1 (Left) shows raw coherence values between pressure and vertical seismic velocity data from the first 30 days in 2014. Figure 1 (right) shows an annual average. They indicate that when pressure is high, coherence can be quite high for frequencies between about 0.01 Hz and 0.05 Hz. Based on this, we focus our analysis on this frequency range, particularly choosing the high-pressure time intervals.

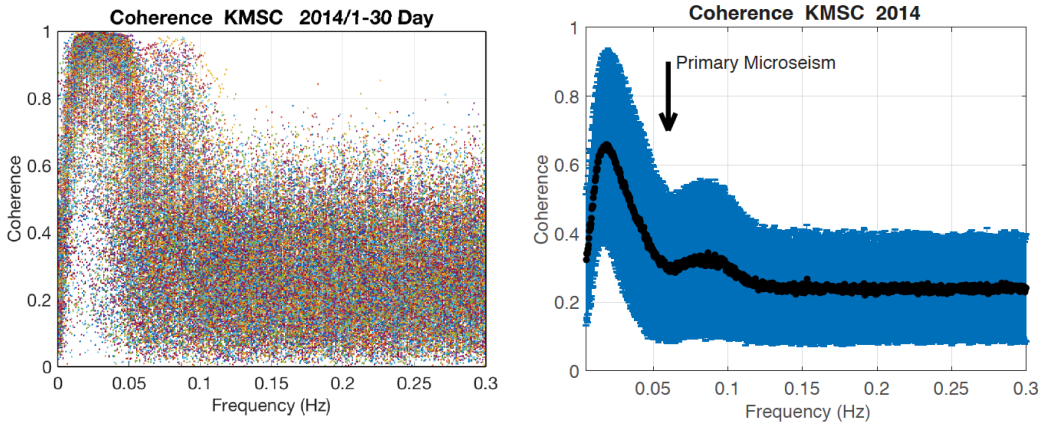

Figure 1: (Left) Raw coherence at station KMSC in South Carolina from the first 30 days in 2014. The coherence between pressure and vertical seismic velocity data was computed for each 1-hour time interval. Different colors mean different 1-hour time series. (Right) Annual average of coherence. Effects of the ocean-generated microseism weakens coherence at about 0.06 Hz, but atmospheric effects exist up to about 0.12 Hz.

Figure 2 (left) shows the seismic PSDs plotted against pressure PSDs at 0.02 Hz for an ErathScope station U57A. Vertical seismic PSDs are in blue and horizontal PSDs (sum of two directions) are in red. Vertical PSDs show a near-constant (flat) range for pressure PSDs below 1 Pa^2/Hz where seismic PSDs do not vary with Pressure PSDs. But above this pressure (1 Pa^2/Hz), the vertical PSD becomes proportional to the pressure PSD, indicating that local pressure becomes the controlling source for seismic noise above about pressure 1 Pa^2/Hz. In the right panel (Figure 2), the time intervals with coherence higher than 0.7 are indicated by green points. High-coherence (green) points are found mainly above 1 Pa^2/Hz and confirms the fact that when surface pressure is the controlling source, pressure and seismic data become highly coherent.

Figure 3 shows phase shifts between pressure and vertical displacement at three stations (bottom panels). It shows that pressure and vertical displacement have opposite signs; when pressure is high, surface is depressed downward and vice versa. The surface is going up and down with surface pressure with opposite signs, as illustrated in Figure 3. In this situation, the solid Earth is responding to surface pressure changes and the ratio $\eta(f) = S_z/S_p$ should give us a measure of its elastic response. From colocated data, we measure this quantity between 0.01 Hz and 0.05 Hz and invert for elasticity of shallow structure.

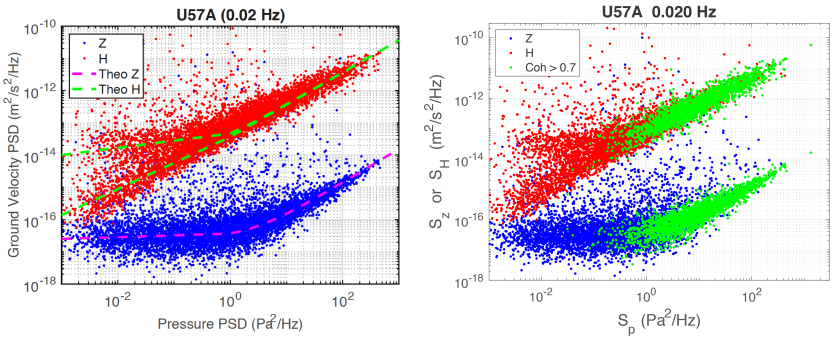

Figure 2: (Left) Seismic velocity PSDs plotted against pressure PSDs at 0.02 Hz. Vertical PSDs in blue and horizontal PSDs (sum of two components) in red. Vertical PSDs have a threshold pressure PSD at about 1 Pa²/Hz above which the vertical PSDs and pressure PSDs become correlated. (Right) Same station with the left panel except that time intervals with coherence higher than 0.7 are indicated by green.

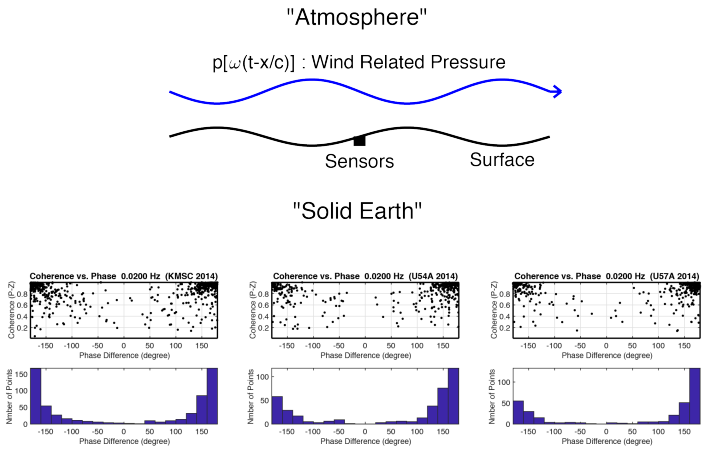

Figure 3: When pressure and vertical data are coherent, phase shifts between vertical displacement and pressure are 180 degrees (shown at three different stations), suggesting the situation in the upper panel. The top panel indicates that when pressure is high, the surface is depressed downward and vice versa. Earth's surface is literally responding to the local pressure.

(2.2) Pressure-Seismic data from 2000's

Figure 4 shows some examples of pressure-seismic plots from the 2000s. These [plots are similar to Figure 2. The key to success of our approach depends on our ability to measure the gradients $\eta(f) = S_Z/S_P$ in these plots. Top two panels for stations BAR and MLAC are the cases that our method works well because coherence computations allow us to identify the relevant time intervals shown in green. They are the times when surface pressure became large and deformed the medium. High coherence indicates that the local pressure variations exceed the effects from other sources of seismic noise (such as ocean waves). There is no problem measuring the gradients in these data because we can focus on green data points.

The bottom two panels in Figure 4 show the cases that our method does not work. We simply cannot find time intervals that show high coherence between pressure and seismic data and there were, unfortunately, many older stations like this.

We investigated by making inquiries to people (at Caltech) who have some knowledge on these stations (GLA and GSC and others). But we could not find out exactly where the pressure sensors were located with respect to seismic sensors; In our view, pressure sensor has to be within 10 m for good coherence (separation in the EarthScope TA is typically 2-3 m at most) and we suspect that pressure sensors at those stations were farther away from seismic sensors for stations.

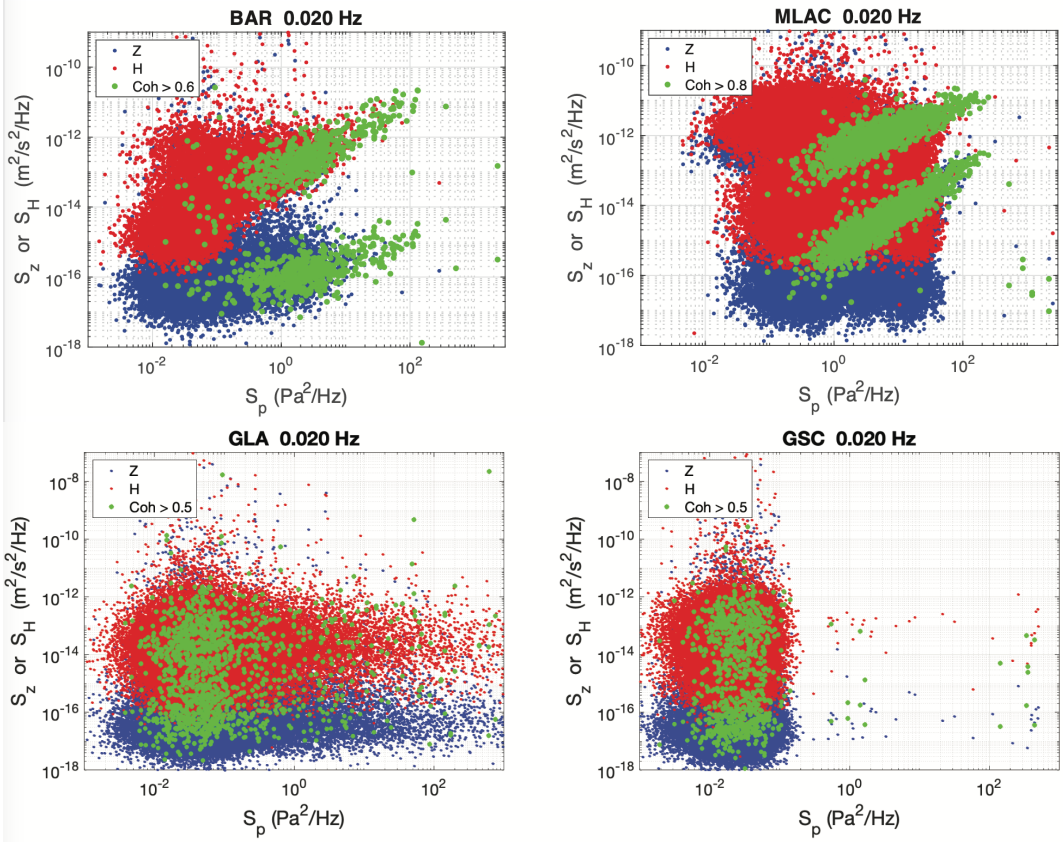

Figure 4: (Upper) Upper panels show examples that our method work as high-coherence time intervals in green can be identified and their gradient S_z/S_P can be measured. (Bottom) Lower panels show that our method clealr does not work. We postulate that pressure sensors were not sufficiently close to seismic sensors.

(2.3) Results for Vs30

After selection of highly coherent data, based on visual examination of pressure-seismic plots of about 62 stations in California, we could estimate shallow structure and thus their Vs30 at 28 statins in the Table. Stations BPH** and TPFO are actually not old stations but are relatively new stations at Pinyon Flat Observatory. It turned out that we could not consgtrain shallow structures at 34 locations out of 62.

We suspect that installation of pressure and seismic sensors were not made sufficiently close. Pressure and seismic sensors were not quite “co-loocated” for our purpose. This may be natural because seismologists usually deal with wavelengths larger than 1 km and differences on the scale of 1-10m are hardly important for most seismological studies. These results shed some light on the limitation of our approach and will be published in a paper that describes the theoretical aspect of our approach.

Table: Shallow structures were derived at the following locations. Vs30 values are from these structures.

Station.	Lat.	Lon.	Elev.	Vs30
214A	31.956	-112.811	543.000	550
BRIB	37.919	-122.152	219.700	350
MHDL	37.842	-122.494	94.500	190
OHLN	38.006	-122.273	-0.500	150
OXMT	37.499	-122.424	208.100	480
SBRN	37.686	-122.411	4.000	310
SVIN	38.033	-122.526	-27.500	199
BAR	32.680	-116.672	529.000	215
MLAC	37.630	-118.836	2162.000	218
NEE	34.825	-114.599	170.000	135
OSI	34.614	-118.724	718.000	290
PAS	34.148	-118.171	314.000	349
SNCC	33.248	-119.524	275.000	242
USC	34.019	-118.286	58.000	145
VTV	34.561	-117.330	843.000	58.
XPFO	33.611	-116.456	1280.000	710
CMW1	37.540	-121.888	214.000	400
CSU1	37.643	-121.940	375.000	390
BPH01	33.611	-116.455	1292.000	738
BPH03	33.610	-116.455	1285.000	890
BPH05	33.612	-116.455	1302.000	979
BPH06	33.611	-116.452	1294.000	1489
BPH07	33.608	-116.455	1275.000	627
BPH09	33.613	-116.460	1295.000	995
BPH10	33.612	-116.452	1300.000	1159
BPH11	33.605	-116.452	1300.000	603
BPH12	33.606	-116.460	1251.000	1359
TPFO	33.606	-116.454	1275.000	1123

3. Publication during 2021-22

During the past year, this grant supported Mr. Jiong Wang and also the publication of the following articles. Dr. Jiong Wang comleted his Ph.D. study in 2021 and is now a postdoctoral scholar at University of Chicago. His major contribution is the creation of Vs30 map based on our method (Figure 5) which will be published in the submitted paper below (Wang and Tanimoto, 2022).

Tanimoto, T. and J. Wang (2021), Incorporating wind information ini the inversion of co-located pressure and seismic data for shallow elastic structure, Journal of Geophysical Research: Solid Earth, 126, e2020JB021162, https://doi.org/10.1029/2018JB017132

Wang, Jiong (2021), Estimating Near-Surface Elastic Structure from Low-Frequency Seismic Noise, Ph.D. thesis, University of California, Santa Barbara, https://escholarship.org/uc/item/22r26284

Wang, J. and T. Tanimoto (2022), Estimating of Vs30 at the EarthScope Transportable Stations by inversion of low-frequency seismic noise, submitted to Journal of Geophysical Research, Solid Earth.

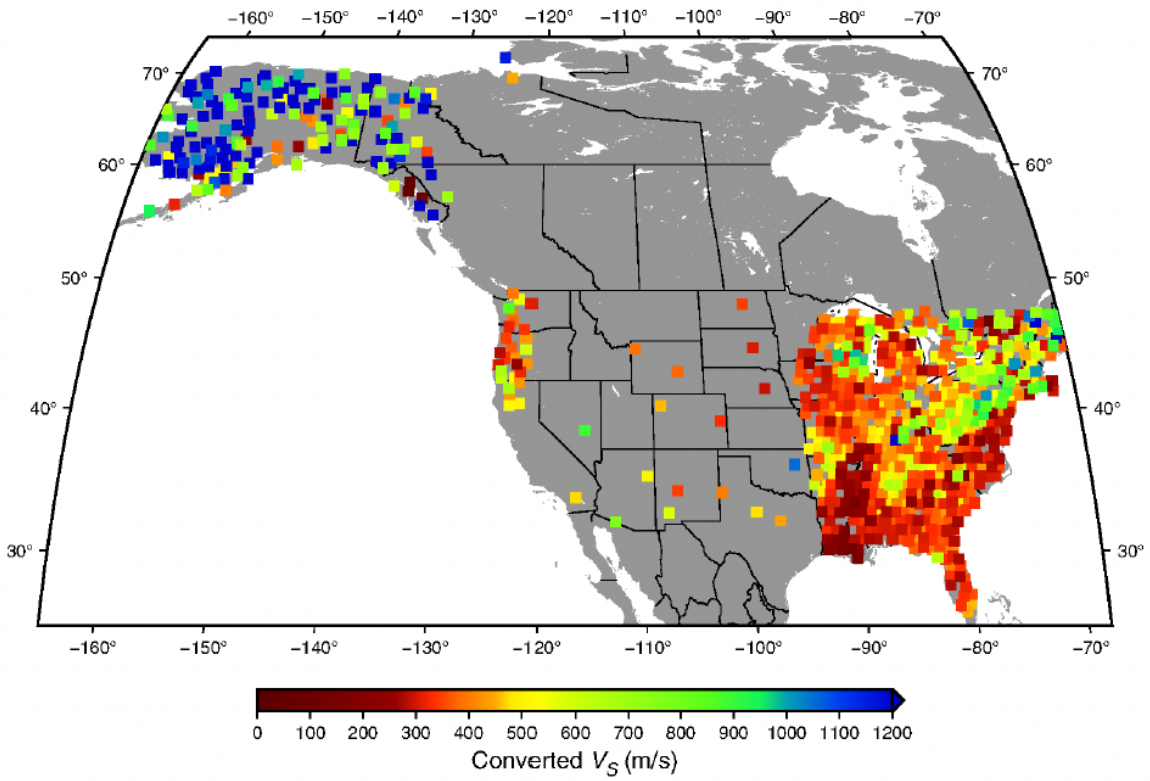

Figure 5: Vs30 based on shallow structures derived from co-located pressure and seismic data.